DRAFT

Transient Processes in Tribology,
Dalmaz, G.; Lubrecht, A.A.; Dowson, D.
& Priest, M. (ed.), Elsevier, 159-164.

The Relationship between Frictional Sound and Lumps Build-up at the Contact Interface in Single-pass Dry Sliding between Aluminium Pin and Flat

Boyko L. Stoimenov[a], Koji Kato[a]

[a] Laboratory of Tribology, Tohoku University
01 Aramaki-Aza-Aoba, Aoba-ku, Sendai 980-8579, JAPAN

Frictional sound is generated whenever two surfaces slide against each other. A number of recent investigations were undertaken to identify the surface conditions which cause uncomfortable sound like squeal noise. In the present study the opposite problem is considered – frictional sound analysis as a means for monitoring the contact.

It is demonstrated that analysis of the waveform of audible sound generated in friction can be used to detect a certain type of surface damage in which material is built up into lumps higher than the original surface asperities.

Audible sound was measured in single-pass sliding of aluminium pin over aluminium flat and load was varied in the range from 1 to 7 N. By comparing power spectral densities (PSD), it was observed that the sound generated in sliding contact was most clearly distinguished from the background noise in the frequency range 450-1000 Hz by difference of about 30 dB. However, such difference was obscured in the time domain, because at frequencies below 450 Hz, the background noise had about 10-15 dB higher spectral density than the one of frictional sound in the range 450 – 1000 Hz. After frequency components below 450 Hz were filtered out from the signal, very short duration significant rises in sound pressure amplitude termed “spikes”, became apparent. It was found that a sound pressure spike is generated due to the build-up of a lump on the flat specimen during sliding. This was confirmed by the matching of the interval between the spikes and the spacing between the lumps. Spikes in the filtered sound signal give a better indication of the lumps build-up, than the leaf spring strain caused by fluctuating friction and normal forces.

The present findings suggest that frictional sound has a potential for use in contact and surface condition monitoring applications.

1. INTRODUCTION

Sound is generated whenever two surfaces slide against each other. Such sound is termed “frictional sound” and it is generated as a response of the system with a certain sound radiation property [1] to excitation at the contact.

Frictional sound can be observed in systems as diverse as the wheel/rail system, the brake system, the gramophone or the violin. In many cases of interest to engineers this sound is not desired and is often described as ‘noise’. There is a large body of research on the reduction or elimination of brake squeal noise [2-4], wheel/rail squeal noise [5-7] and tyre noise [8-10].

A number of recent investigations were undertaken to identify the contact conditions which cause squeal noise generation [2-3,11-13]. In those studies, the general approach was to observe the surface damage after a number of sliding cycles and relate it to long-time averaged sound pressure level or to the presence or lack of squeal.

But the opposite problem of using frictional sound as a means for monitoring the contact is rarely considered. A rare example is the tool proposed by Othman et al. [14] for quick approximate measurements of average surface roughness by using dry friction noise.

At present there appear to be no studies on monitoring and diagnosing surface damage based on audible sound.

The present study demonstrates how analysis of the waveform of audible sound generated in friction can be used to detect a certain type of surface damage in which material is built up into lumps higher than the original surface asperities.

2. EXPERIMENTAL APPARATUS AND PROCEDURE

Experiments were conducted on the apparatus shown in (Fig.1), in which frictional sound was generated by the contact of a pin on a flat bar, attached to a moving stage.

The specimens used in the test were made of aluminium alloy JIS-5052 (ANSI analogue Aluminium 5052–H34), having Young's modulus E = 70 GPa, tensile yield stress Y = 216 MPa and Poisson's ratio $\nu = 0.33$. Pin specimens with tip radius 4 mm were polished to RMS surface roughness in the range of Rq = 30 – 40 nm, while the flat specimen had RMS roughness Rq = 0.86 μm. The profile of the flat specimen was measured over a length of 95 mm before the test and after test along the wear scar. Long wavelength characteristics of the profile were removed in both cases by a Gaussian filter as specified in the ISO11562:1996 standard [15], having cut-off wavelength of 8 mm. The initial surface profile is shown in Fig. 2.

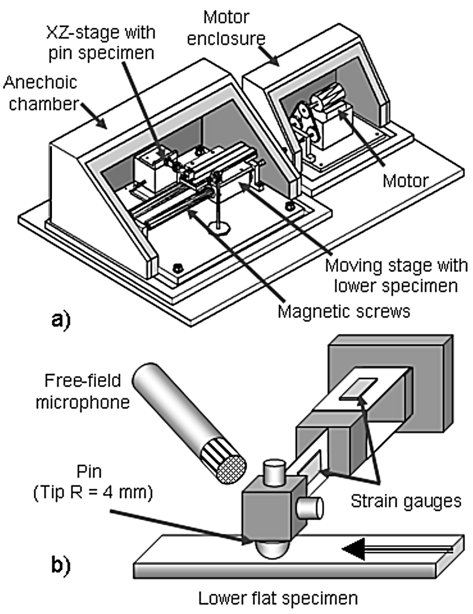

Figure 1. Experimental apparatus: a) overview; b) close-up on the specimens.

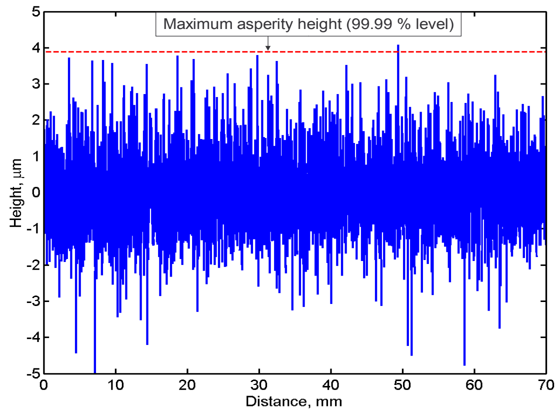

Figure 2. Profile of the flat specimen before test.

On each new test, new pins were used on a fresh portion of the flat specimen. Before testing the specimens were thoroughly cleaned with ethanol, degreased with acetone, and then again cleaned with ethanol. Finally, they were wiped dry with lint-free tissue paper.

The pin-holder was supported by crossed leaf springs bending in normal and in tangential direction respectively. Normal load was applied by the elastic deformation of the normal leaf spring when the XZ-stage was lowered down. The forces in the leaf springs were measured by pairs of strain gauges.

The sound was measured by a free-field microphone, placed at about 8.5 cm from the centre of the pin-holder. Antialiasing low-pass filter with cut-off frequency set to 6000 Hz was placed before the A-D converter used to acquire the signals into a personal computer.

To reduce the background noise levels, the motor was placed in a separate sound insulated compartment and magnetic screws were used to move the stage on which the flat specimen was mounted. The test chamber was covered with sound-absorbing material on the inside to eliminate sound reflections and create free field conditions.

All experiments were done in air at room temperature and relative humidity 30-60 %.

A series of tests were carried out for sliding speeds of 20 mm/s and load setting from 1 to7 N incremented in steps of 1 N. For the selected material and pin radius, based on criteria commonly accepted for Hertz contact [16], the onset of plastic deformation under static load was determined to occur at 1.82 N, and fully plastic deformation - at 40.0 N. The average load values observed in the experiment differ slightly from the pre-set values. The following section shows only some representative data.

3. RESULTS

Some representative signals during sliding are shown in Fig.3. The force in the tangential leaf spring fluctuates in pattern similar to stick-slip and as the contact load is increased, the fluctuations also increase. The sound data looks very noisy and it is difficult to distinguish specific features, but it can be seen that increase of contact load also resulted in increase in sound pressure amplitude.

When the recorded sound signals were played back, some characteristic pulses could be distinguished by hearing, which were not obvious from visual inspection of the sound data (Fig. 3). This suggested that the sound from the contact was masked by large amplitude noise.

Fig. 4 is a plot of the power spectral density (PSD) functions of sound generated by the stage motion when the specimens are not in contact and under average contact load of 0.9, 3.0 and 4.9 N. The frequency range in which the difference between stage noise and sound from the contact is largest (about 30 dB), and possibly contains most information about the contact is from about 450 Hz to about 1000 Hz. At higher frequencies above 5500 Hz, the power spectral density reduction is due to the anti-aliasing analogue filter in the data-acquisition system. At frequencies lower than 450 Hz, the PSD of background noise was about 10-15 dB higher than the PSD of frictional sound in the range 450 - 1000Hz, thus making the difference indistinguishable in the plots of sound pressure as a function of time.

In order to remove such low frequency noise the raw data were filtered by cutting out the frequencies below 447 Hz (lower limit of the 27th 1/3 octave frequency band). The designed filter was a Chebyshev type II, high-pass filter with pass-band starting at 447 Hz, transition-band was 400 - 447 Hz, attenuation in the stop-band 30 dB and pass-band ripple 1 dB.

The filtered sound data is shown in Fig. 5. There are clearly defined spikes, which are very short duration (10-20 ms) significant rises in sound pressure amplitude (several times to more than 100 times larger than the average sound amplitude). As the contact load increased the height of the spikes also increased.

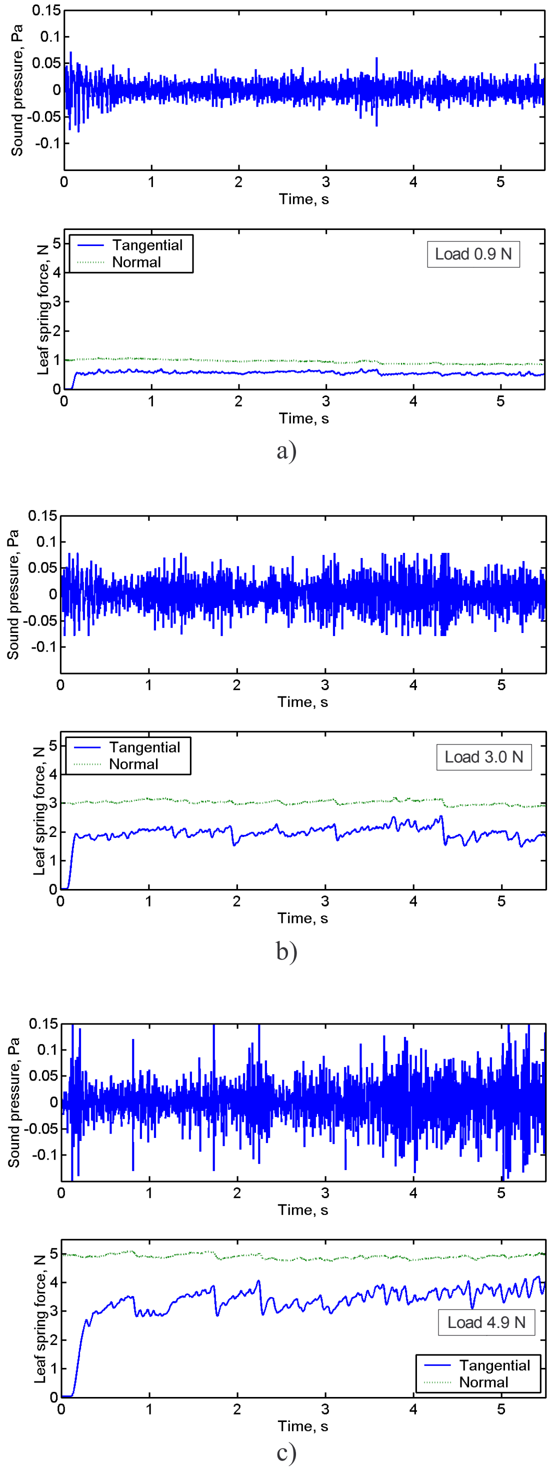

Figure 3. Frictional sound and leaf spring forces under average load of: a) 0.9 N, b) 3.0 N and c) 4.9 N.

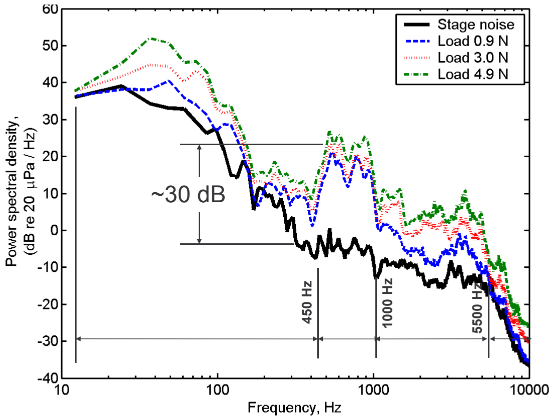

Figure 4. Power spectral density of stage motion sound and friction sound from the pin/flat contact.

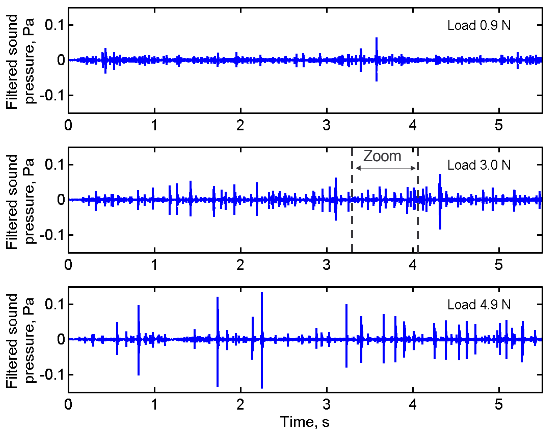

Figure 5. High-pass filtered sound pressure.

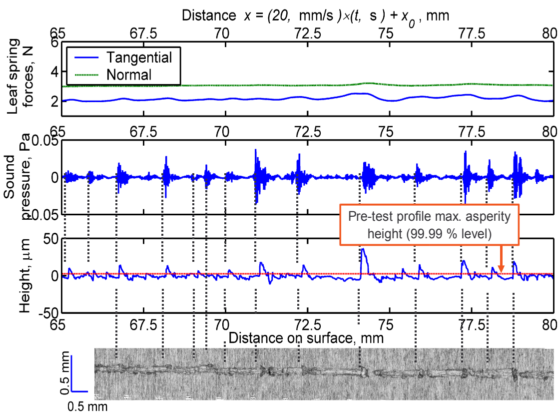

Figure 6. Zoomed-up portion of sound pressure signal at 3.0 N together with wear scar profile, scar photograph and strain-gauge measured elastic forces.

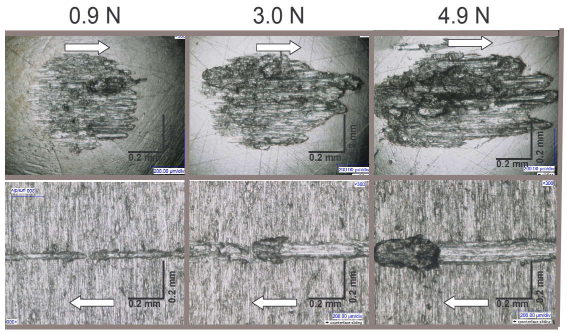

Figure 7. Surface damage on pin and flat. Arrows show counterface sliding direction.

Fig. 6 shows a short portion of the signals recorded during sliding under average load of 3.0 N, the corresponding profile of the wear scar and photographs of the surface as observed by optical microscope. The recorded signals are plotted as a function of sliding distance calculated from time and sliding speed. The short distance during which the stage accelerates in the beginning of sliding is ignored.

From the figure it is seen that sound pressure spikes correspond to the highest portions of the profile of the wear scar. Almost all such portions protrude above the level containing 99.99% of the original profile heights, which means that they were built-up during sliding. From the photograph of the wear scar it is seen that such built-up material has the shape of a lump. Fig. 7 shows lumps on the flat specimen and the corresponding pin tip damage after sliding at average loads of 0.9, 3.0 and 4.9 N.

When the filtered sound signal is compared to the signals measured by the strain gauges on the leaf springs (Fig. 6) it is seen that sound contains higher detail and is more easily correlated to the surface damage.

When the correspondence of sound spikes and built-up lumps is considered, ideally, we would like to match every lump on the surface with a particular spike in the sound pressure. However, over a longer sliding distance, the number of lumps and spikes becomes very large and this creates a difficulty in doing the match manually.

This is why we considered only spikes defined by sound pressure amplitude larger than 95% of the measured sound pressure data during the whole sliding, and lumps with height larger than 95% of the wear scar profile height data. The lines marking these levels are shown in the figure (Fig. 8).

The spikes and lumps selected in this way match very well for the length of 65 mm. This confirms that the spikes are generated due to the build-up of lumps on the surface.

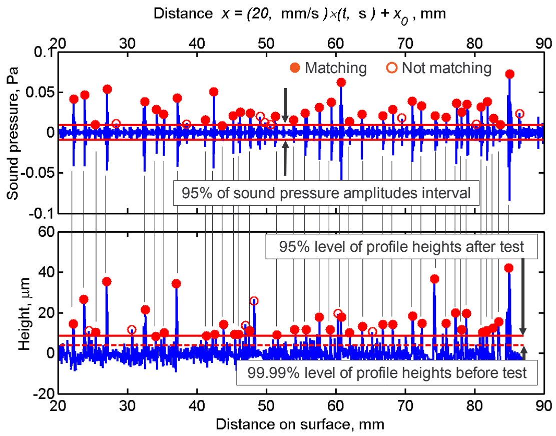

Figure 8. Matching of sound pressure spikes and built-up lumps.

4. DISCUSSION

During sliding of the pin over the flat specimen surface, a wedge is formed on the pin tip (Fig. 9). As the sliding continues, the wedge grows and at certain point suddenly sticks to the flat specimen surface. At that time a sudden impulse acts on the pin and on the flat specimen, exciting the pin-holder and the sliding stage into vibration, which is perceived as a sound pressure spike. This is confirmed by measurements of pin-holder acceleration in normal and tangential direction (Fig. 10).

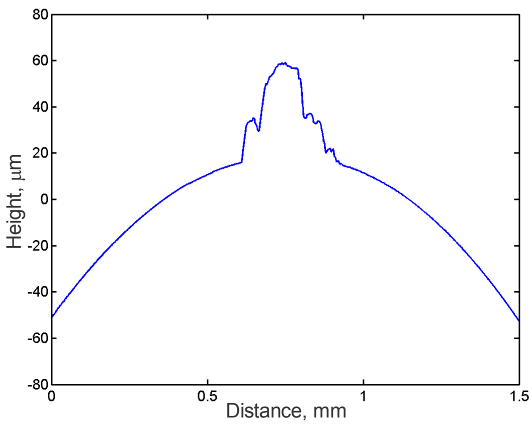

Figure 9. Pin tip after test at 3.0 N.

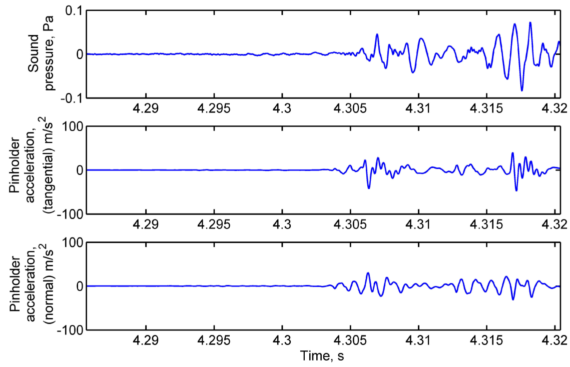

Figure 10. Pin-holder acceleration and sound pressure.

5. CONCLUSIONS

Audible sound was measured in single-pass sliding of aluminium pin (tip radius 4 mm) over aluminium flat with sliding speed of 20 mm/s and load varied in the range from 1 to 7 N.

The sound pressure signals were filtered to remove the high amplitude (30-50 dB) low frequency (<450 Hz) noise which obscured the low amplitude (20-30 dB) sound from the contact, having frequencies between 450 and 1000 Hz. After such filtering, very short duration (10-20 ms) significant rises in amplitude (several times to more than 100 times larger than the average sound amplitude), termed “spikes” became obvious in the sound pressure signal.

1. It was found that a sound pressure spike is generated during sliding due to the build up at the contact interface of a lump, which has height above the original pre-test profile maximum asperity height. This was confirmed by the matching of the interval between the spikes and the spacing between the lumps.

2. Spikes in the filtered sound signal give a better indication of the lumps build-up than the leaf spring strain caused by fluctuating friction and normal forces.

The present findings show that frictional sound is very well correlated to surface damage and sliding conditions and has a potential for application in advanced surface and contact condition monitoring systems.

REFERENCES

[1] Stoimenov, B.L., Kato, K. and Adachi, K. (2002) Sound Radiation Property of a Tribo-system. Proc. 2nd ASIATRIB Conference, Jeju Island, Korea, Oct 21-24, 383-384.

[2] Eriksson, M., Bergman, F. and Jacobson, S. (1999) Surface Characterisation of Brake Pads after Running under Silent and Squealing Conditions. Wear, 232, 163-167.

[3] Bergman, F., Eriksson, M. and Jacobson, S. (1999) Influence of Disc Topography on Generation of Brake Squeal. Wear, 225-229, 621-628.

[4] Papinniemi, A., Lai, J.C., Zhao, J. and Loader, L. (2002) Brake Squeal: a Literature Review. Applied Acoustics, 63, 391-400.

[5] Remington, P.J. (1985) Wheel/Rail Squeal and Impact Noise: What Do We Know? What Don't We Know? Where Do We Go From Here? Journal of Sound and Vibration, 116, 339-353.

[6] Obara, T., Ohyama, T. and Kato, K. (2000). Influence of Wheel Corrugation on Rolling Noise. International Tribology Conference, Nagasaki, 159.

[7] Heckl, M.A. (2000) Curve Squeal of Train Wheels, Part 2: Which Wheel Modes Are Prone to Squeal? J. Sound and Vibration, 229, 695-707.

[8] Larsson, K., Barrelet, S. and Kropp, W. (2002) The modelling of the dynamic behaviour of tyre tread blocks. Applied Acoustics, 63, 659-677.

[9] Kropp, W. (1989) Structure-borne sound of a smooth tyre. Applied Acoustics 72, 28–32.

[10] Kim, G. J., Holland,K. R. and Lalor, N. (1997) Identification of the airborne component of tyre-induced vehicle interior noise. Applied Acoustics 51, 141-156.

[11] Yokoi, M. and Nakai, M. (1979) A Fundamental Study on Frictional Noise (1st report - The generating mechanism of rubbing noise and squeal noise). Bulletin of the JSME, 22, 1665-1671.

[12] Jibiki, T., Shima, M., Akita, H. and Tamura, M. (2001) A Basic Study of Friction Noise Caused by Fretting. Wear, 251, 1492-1503.

[13] Guangxiong, C., Zhongrong, Z., Kapsa, P. and Vincent, L. (2002) Effect of surface topography on formation of squeal under reciprocating sliding. Wear, 253, 411-423.

[14] Othman, M.O. and Elkholy, A.H. (1990) Surface Roughness Measurement Using Dry Friction Noise. Experimental Mechanics, 47, 309-312.

[15] ISO 11562:1996 "Geometrical Product Specifications (GPS) - Surface texture: Profile method - Metrological characteristics of phase correct filters."

[16] Bhushan, B., "Principles and applications of Tribology", Wiley, New York, 1999.